

Supporting Information

Redox-responsive Supramolecular Amphiphilics Based on Pillar[5]arene for Enhanced Photodynamic Therapy

Ye Chen, Leilei Rui, Lichao Liu, Weian Zhang*

Shanghai Key Laboratory of Functional Materials Chemistry, East China University of Science and Technology, 130 Meilong Road, Shanghai 200237, P. R. China

**Correspondence to: Weian Zhang (wazhang@ecust.edu.cn)*

1. Synthesis of PEG-P[5]A

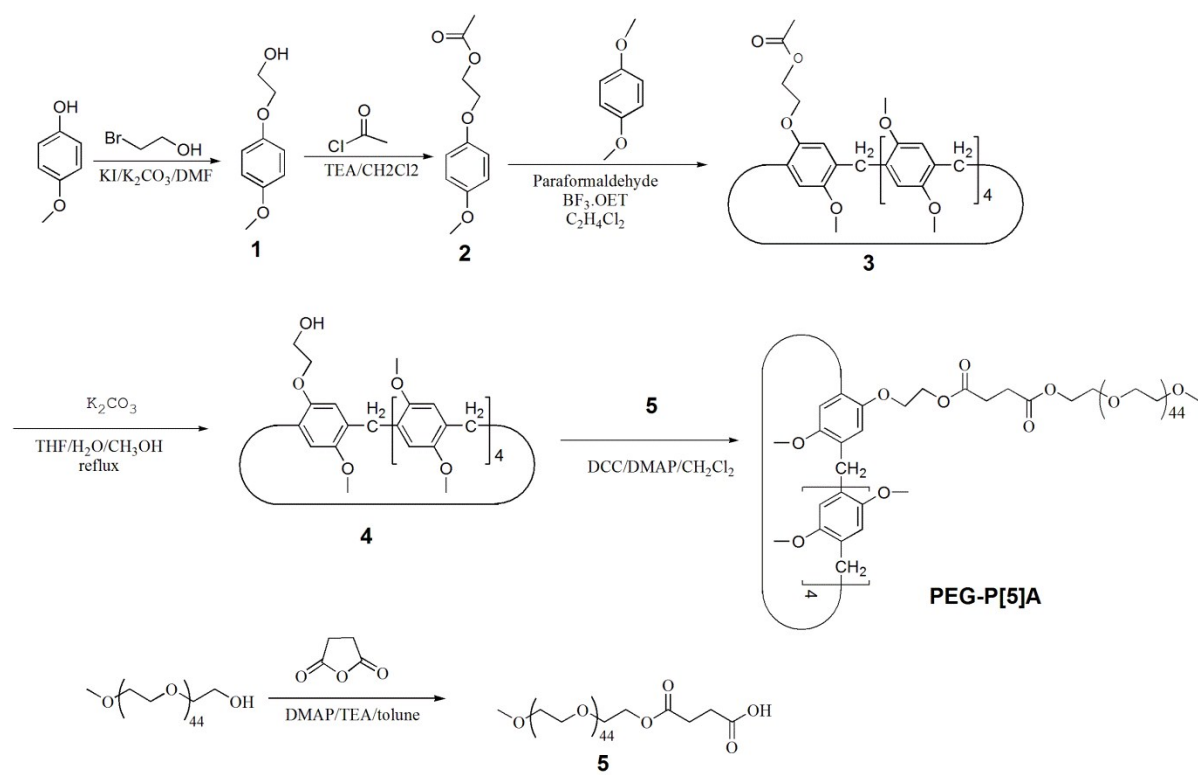
Poly(ethylene glycol)-functionalized pillar[5]arene (PEG-P[5]A) was prepared according to our previous work¹ and the synthetic procedure was shown in **Scheme. S1**.

2. Synthesis of TPPC6-SS-COOH

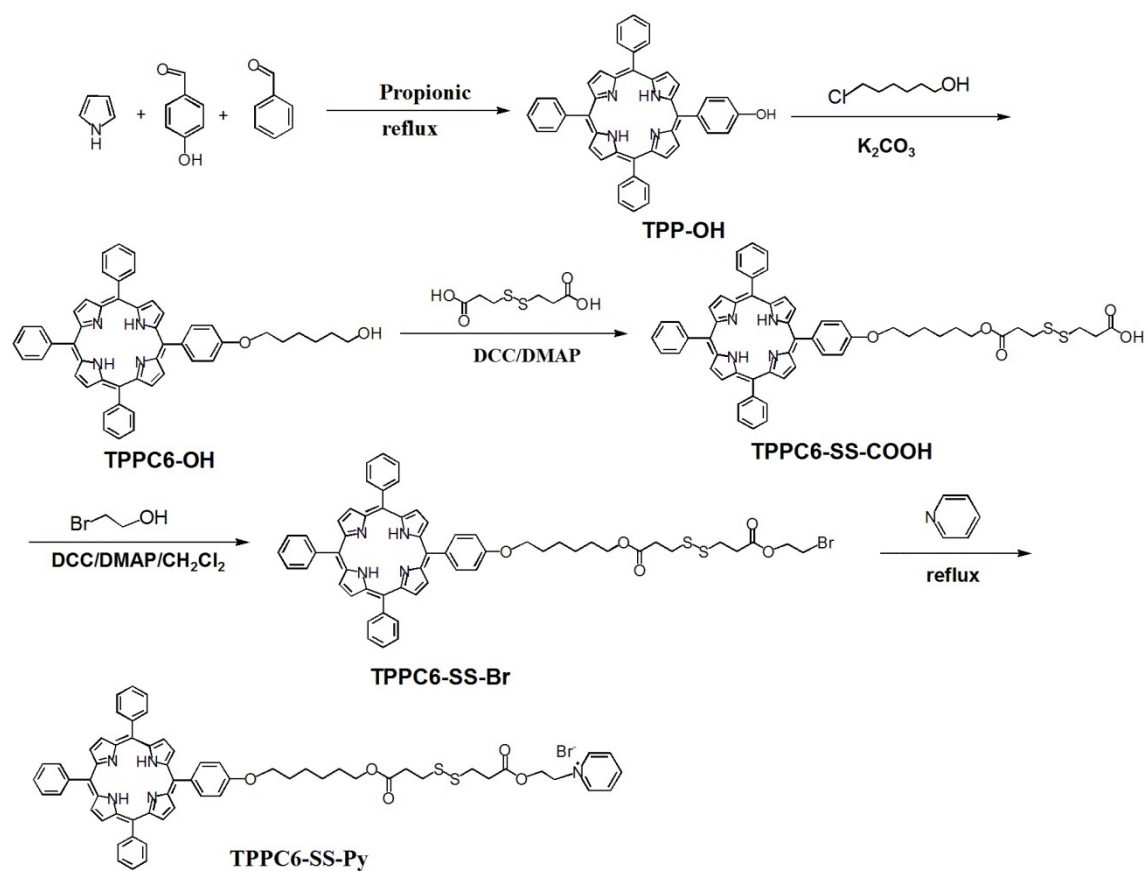
The carboxyl-terminated porphyrin (TPPC6-SS-COOH) was prepared according to our previous work² and TPPC6-SS-COOH was further used to synthesize pyridinium-terminated porphyrin derivative bearing a disulfide bond (TPPC6-SS-Py), as shown in **Scheme. S2**.

3. Synthesis of the Model Guest Compound (**G_M**)

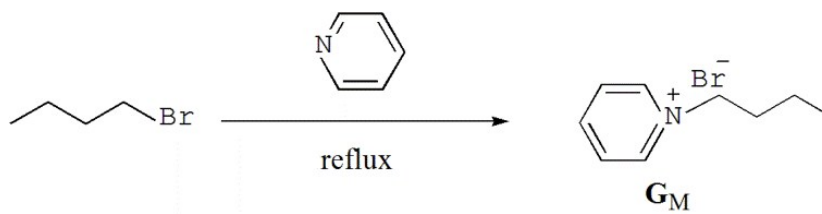
1-Bromobutane (0.685 g, 5 mmol) and excessive amount of pyridine (0.5 mL, 6 mmol) were refluxed in acetone at 70 °C for 1 day. After the solvent was removed under vacuum, the product **G_M**, *N*-butyl pyridinium bromide was obtained as a yellow solid (0.98 g, 90%). ¹H NMR (400 MHz, D₂O) δ (ppm): 9.47 (d, 2H, pyridinium-H), 8.69 (t, 1H, pyridinium-H), 8.18 (m, 2H, pyridinium-H), 5.03 (t, 2H, N-CH₂-), 2.02 (m, 2H, N-CH₂-CH₂-), 1.51 (m, 2H, N-(CH₂)₂-CH₂-), 1.01 (t, 3H, -CH₃) (**Fig. S15**).



Scheme. S1 Synthetic route of PEG-P[5]A



Scheme. S2 Synthetic route of TPPC6-SS-Py



Scheme. S3 Synthetic route of G_M

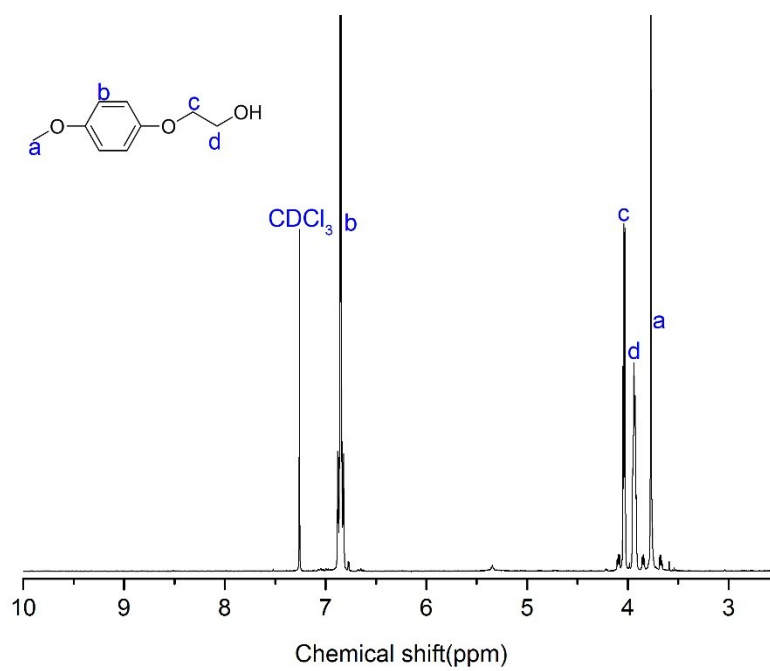


Fig. S1 ^1H NMR spectrum of **1**

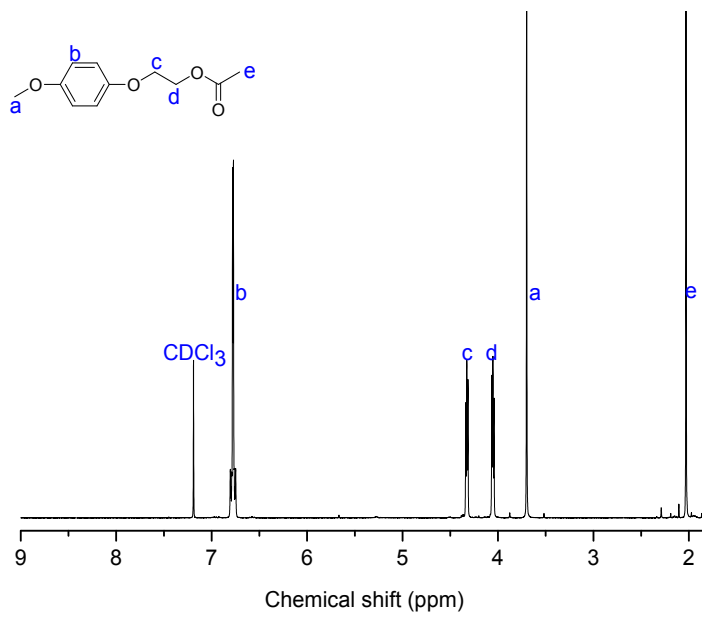


Fig. S2 ¹H NMR spectrum of 2

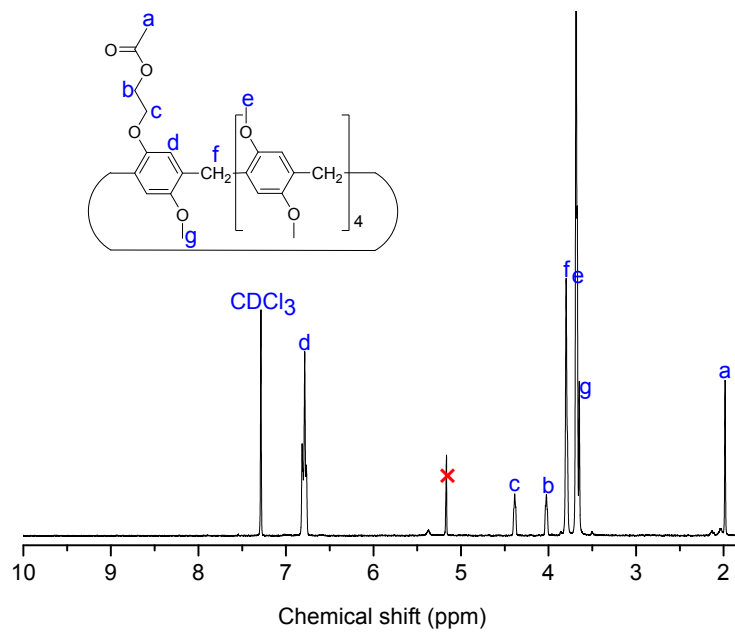


Fig. S3 ¹H NMR spectrum of 3

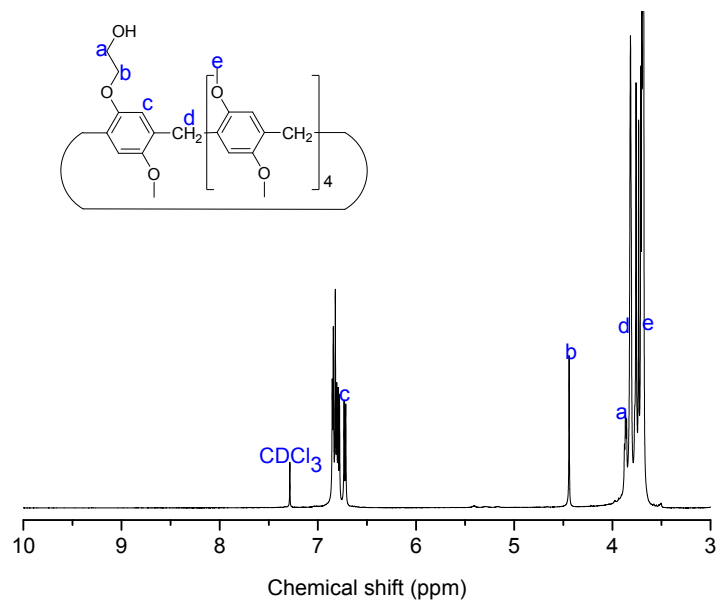


Fig. S4 ¹H NMR spectrum of **4**

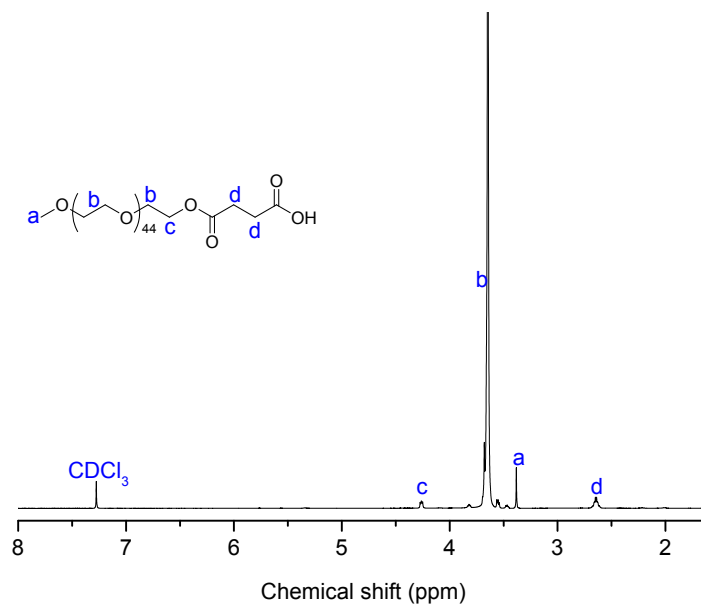


Fig. S5 ¹H NMR spectrum of **5**

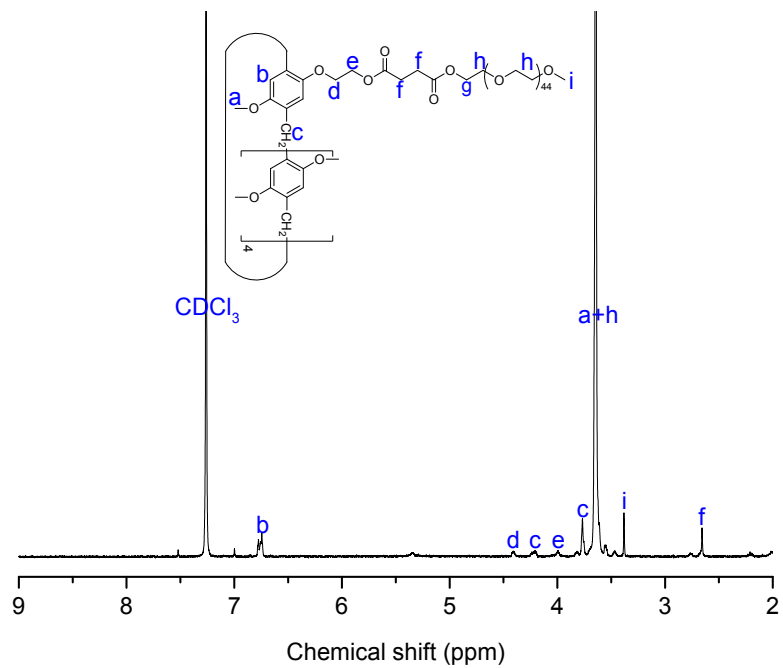


Fig. S6 ^1H NMR spectrum of **PEG-P[5]A**

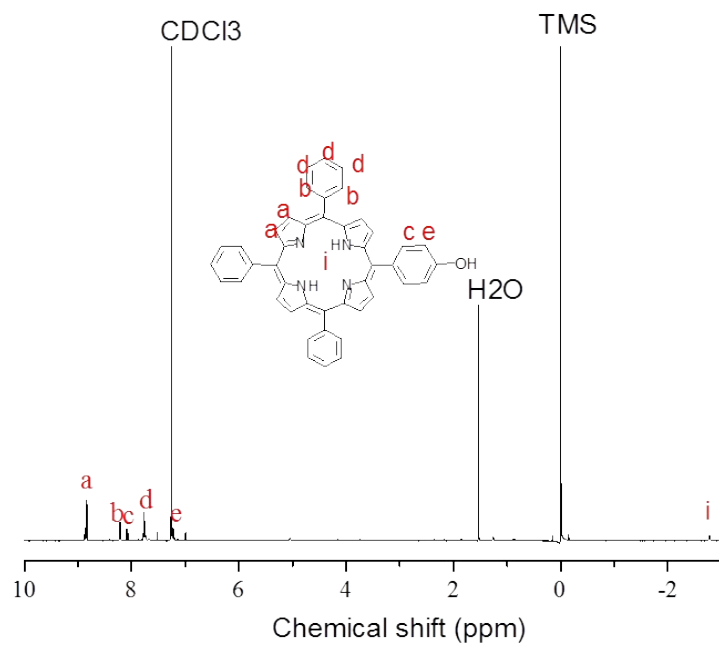


Fig. S7 ^1H NMR spectrum of **TPP-OH**

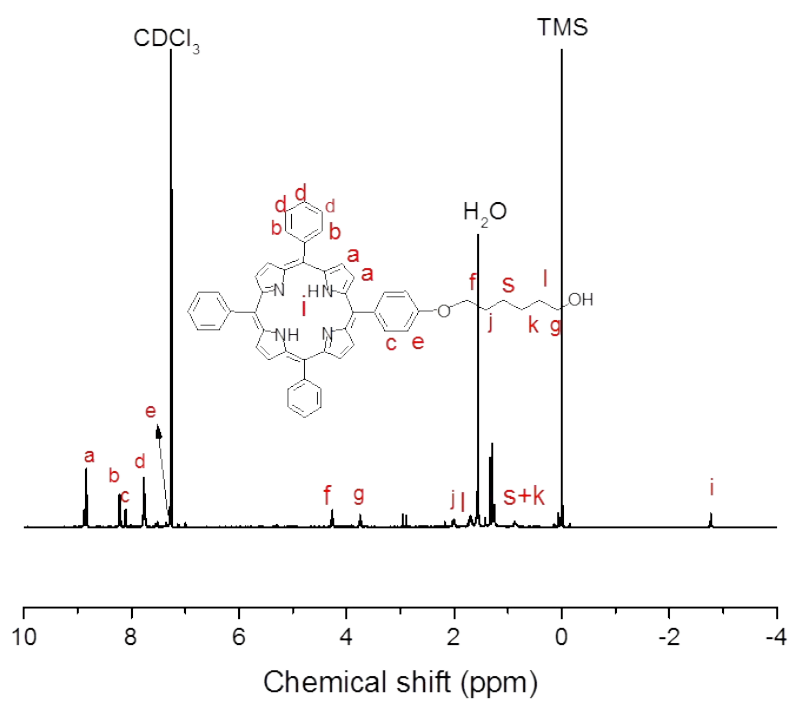


Fig. S8 ¹H NMR spectrum of **TPPC6-OH**

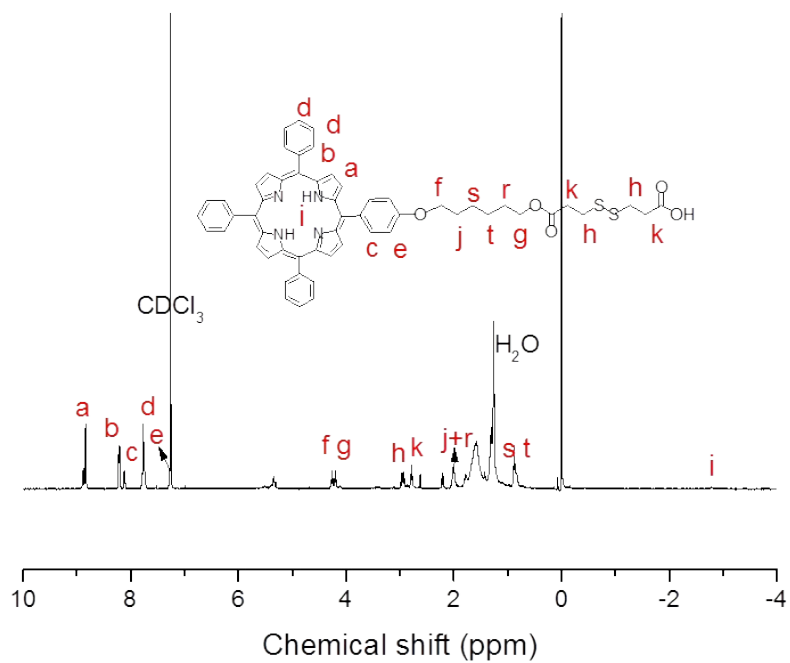


Fig. S9 ¹H NMR spectrum of **TPPC6-SS-COOH**

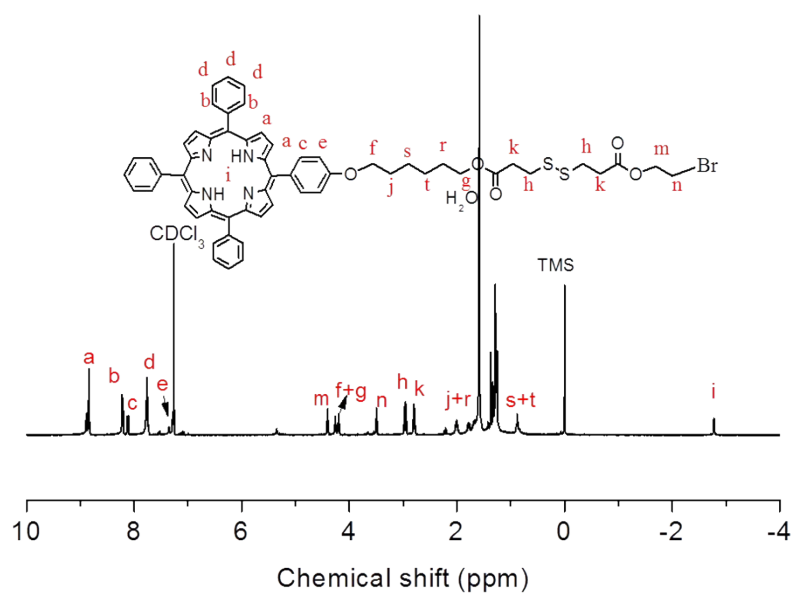


Fig. S10 ^1H NMR spectrum of TPPC6-SS-Br

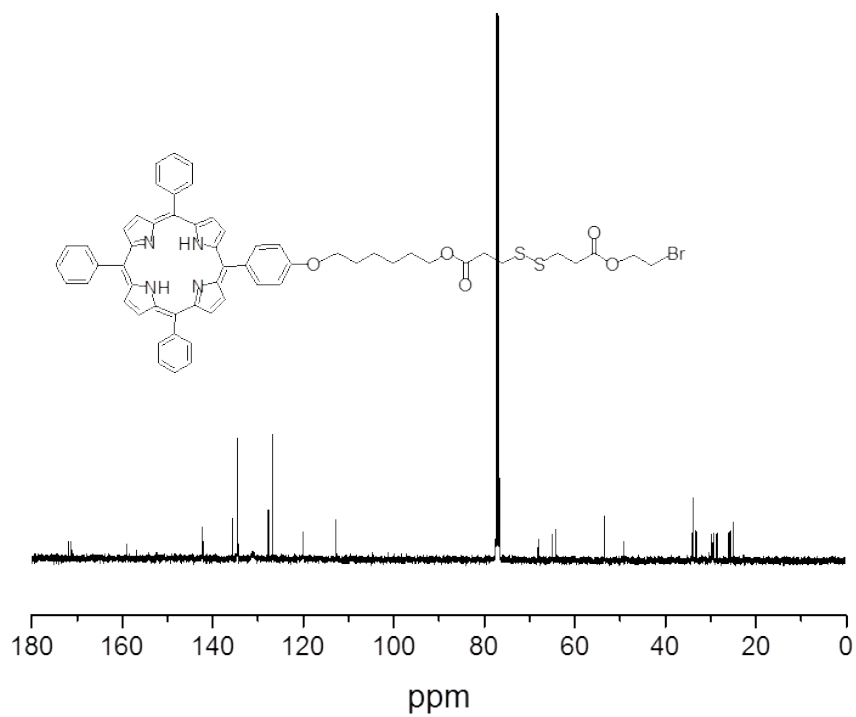


Fig. S11 ^{13}C NMR spectrum of TPPC6-SS-Br in CDCl_3

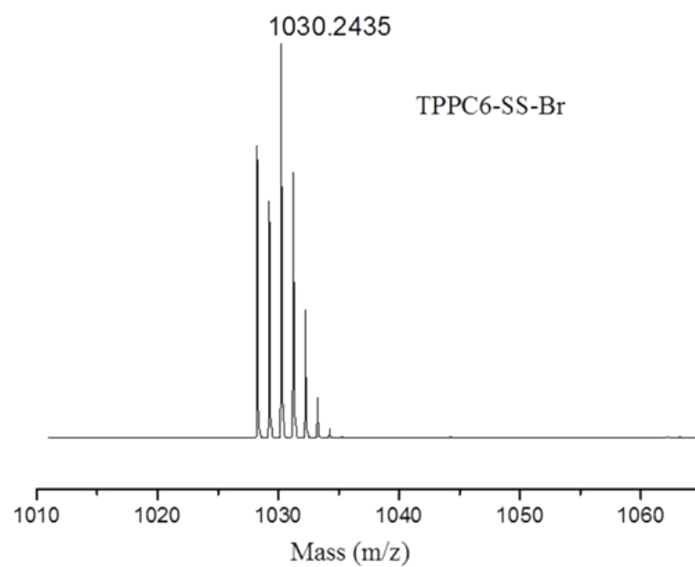


Fig. S12 MALDI-TOF-MS spectrum for **TPPC6-SS-Br**, calcd for $C_{58}H_{53}BrN_4O_5S_2$, 1030.10; found: 1030.2435.

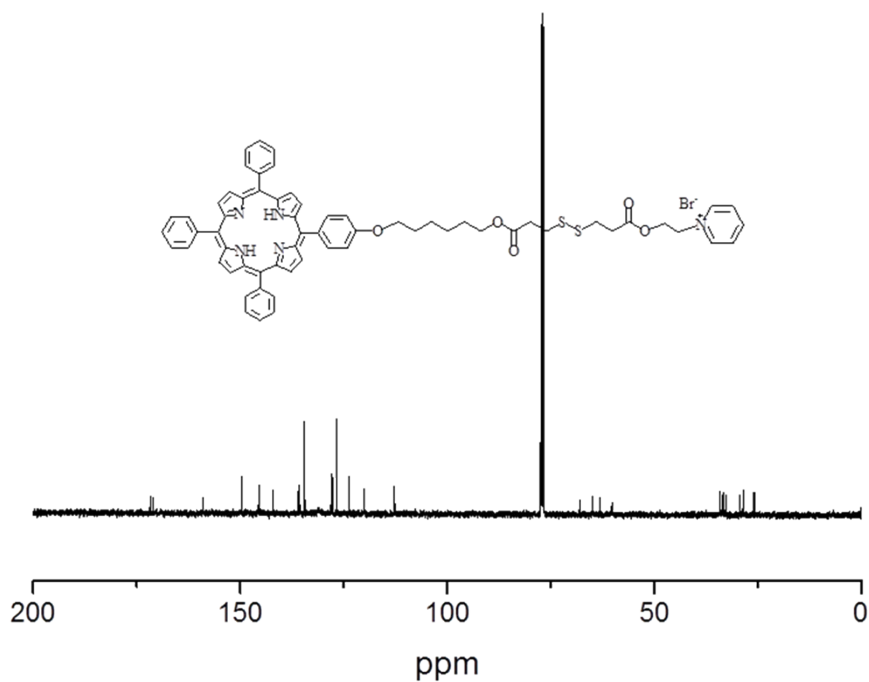


Fig. S13 ^{13}C NMR spectrum of **TPPC6-SS-Py** in $CDCl_3$

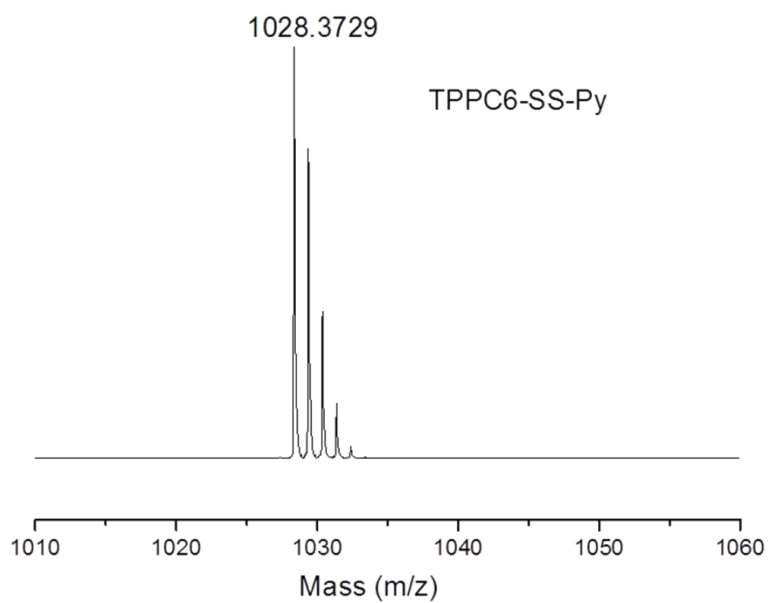


Fig. S14 MALDI-TOF-MS spectrum of TPPC6-SS-Py, calcd for $[M-Br]^+$: $C_{63}H_{58}N_5O_5S_2$, 1028.39; found: 1028.3729.

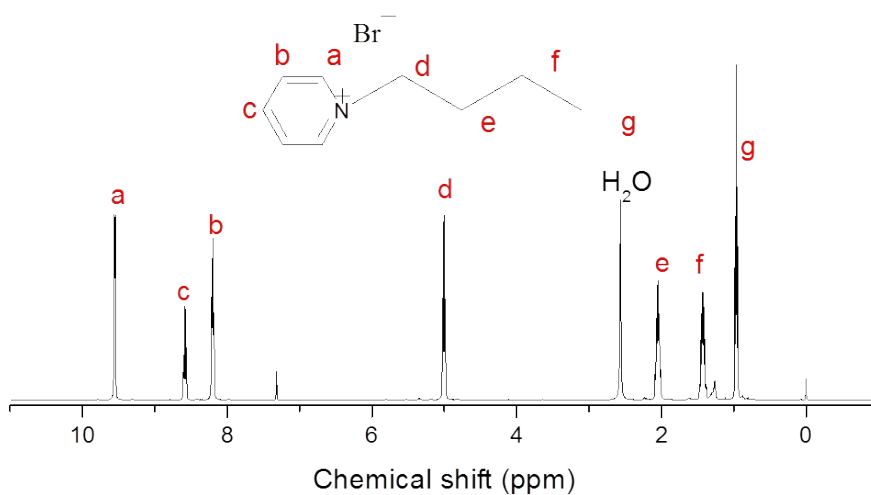


Fig. S15 1H NMR spectrum of G_M

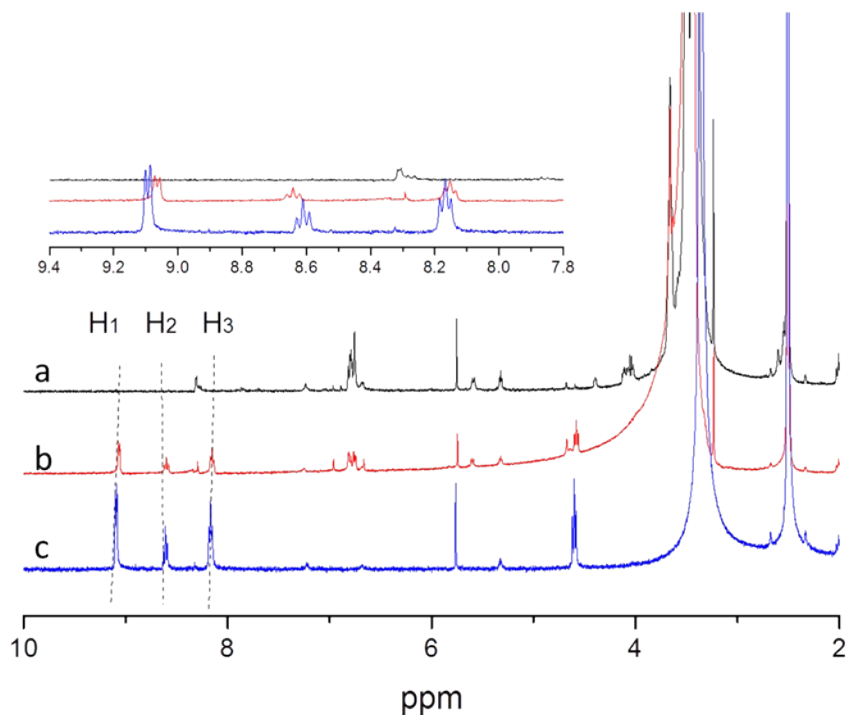


Fig. S16 Partial ¹H NMR spectra (400 MHz, DMSO-*d*₆) of a) PEG-P[5]A (2 mM), b) a 1:1 mixture of PEG-P[5]A and G_M and c) G_M (2 mM).

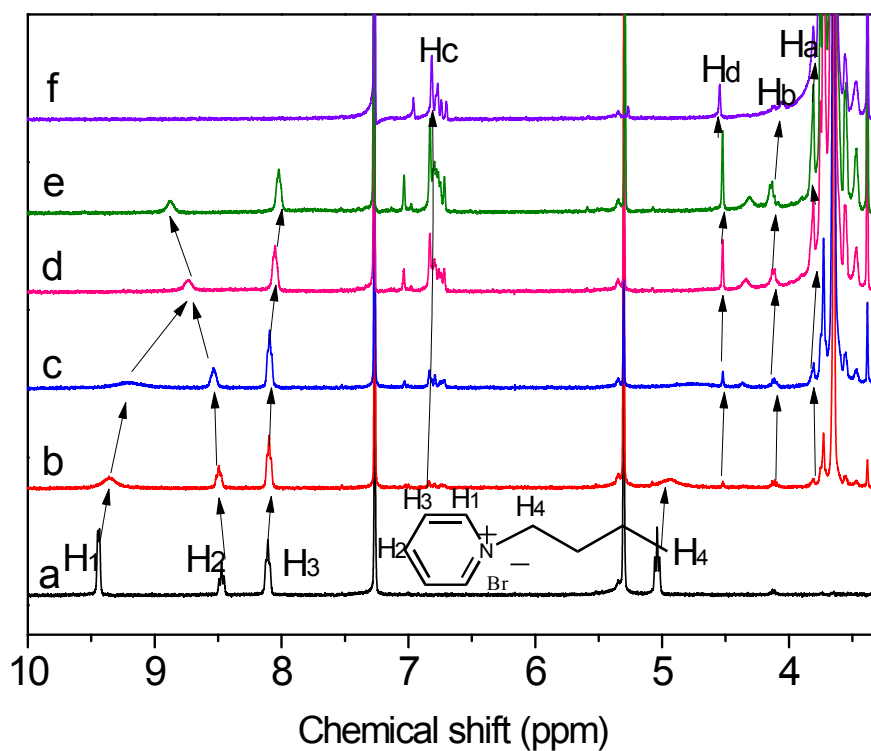


Fig. S17 Partial ¹H NMR spectra (400 MHz, CDCl₃) of G_M at a constant concentration of 2 mM with different concentrations of PEG-P[5]A: (a) 0.00 mM, (b) 0.5 mM, (c) 1.00 mM, (d) 2.00 mM, (e) 4.00 mM, and (f) only PEG-P[5]A at 2 mM.

Investigation of the Interactions between PEG-P[5]A and G_M

To determine the association constant for the complexation between PEG-P[5]A and G_M , fluorescence titration experiments were carried out in solutions which had a constant concentration of PEG-P[5]A (2.5×10^{-5} M) and varying concentrations of G_M . By a non-linear curve-fitting method, the association constant (K_a) of PEG-P[5]A \rightarrow G_M was estimated.³

The non-linear curve-fittings were based on the equation:

$$\Delta F = (\Delta F_\infty/[H]_0) (0.5[G]_0 + 0.5([H]_0 + 1/K_a) - (0.5 ([G]_0^2 + (2[G]_0(1/K_a - [H]_0) + (1/K_a + [H]_0)^2)^{0.5})) \quad (\text{eq. 1})$$

Where ΔF is the fluorescence intensity changes at 330 nm at $[H]_0$, ΔF_∞ is the fluorescence intensity changes at 330 nm when PEG-P[5]A is completely complexed, $[G]_0$ is the initial concentration of G_M , and $[H]_0$ is the fixed initial concentration of PEG-P[5]A.

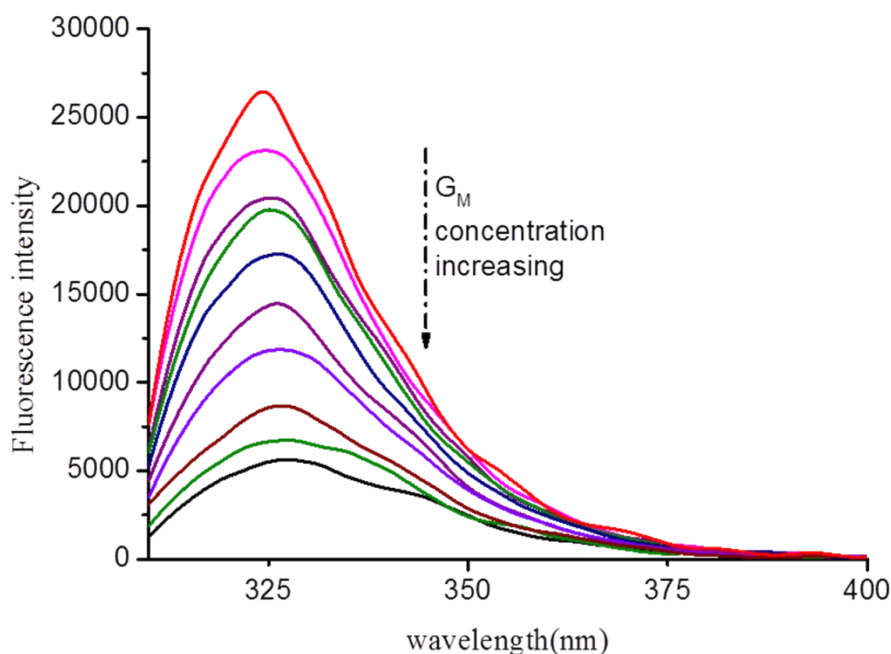


Fig. S18 Fluorescence spectra of PEG-P[5]A (2.5×10^{-5} M) upon addition of G_M (0 - 14.5×10^{-5} M) in DMF at room temperature. Upon addition of G_M , emission from PEG-P[5]A was quenched, indicating the formation of the PEG-P[5]A- G_M complex.

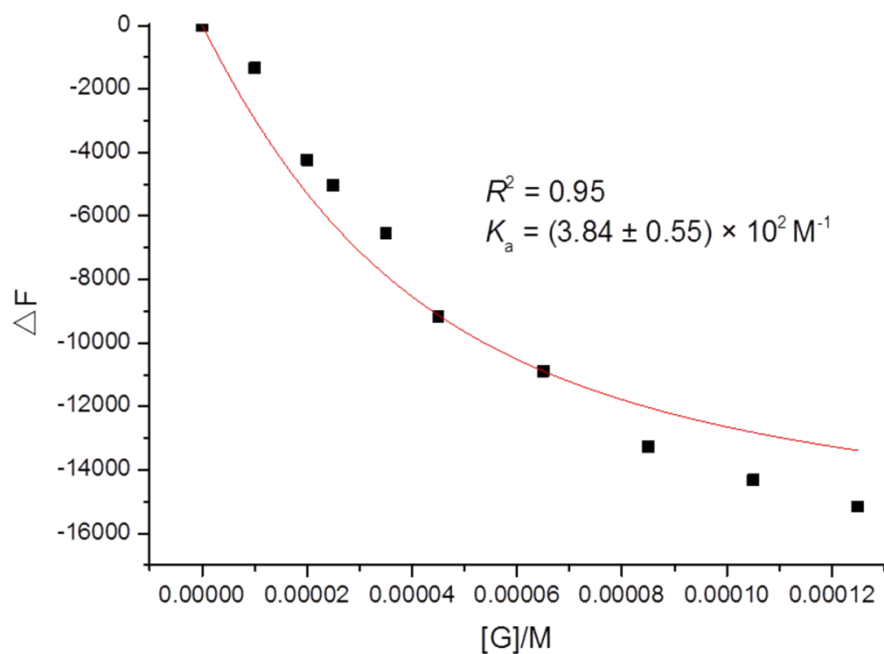


Fig. S19 The fluorescence changes of PEG-P[5]A upon addition of G_M . The red solid line was obtained from the non-linear curve-fitting using eq. 1.

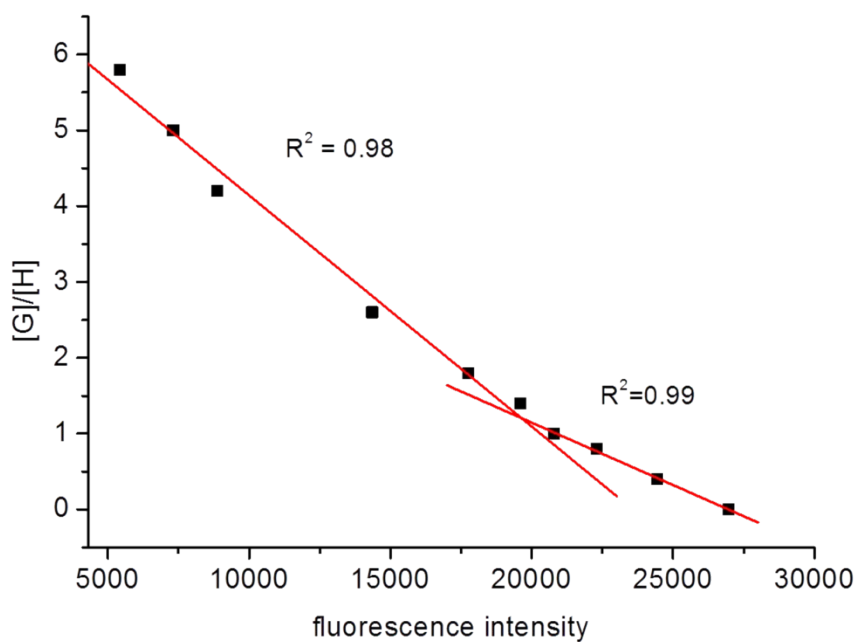


Fig. S20 Mole ratio plot for PEG-P[5]A and G_M , indicating a 1:1 stoichiometry.

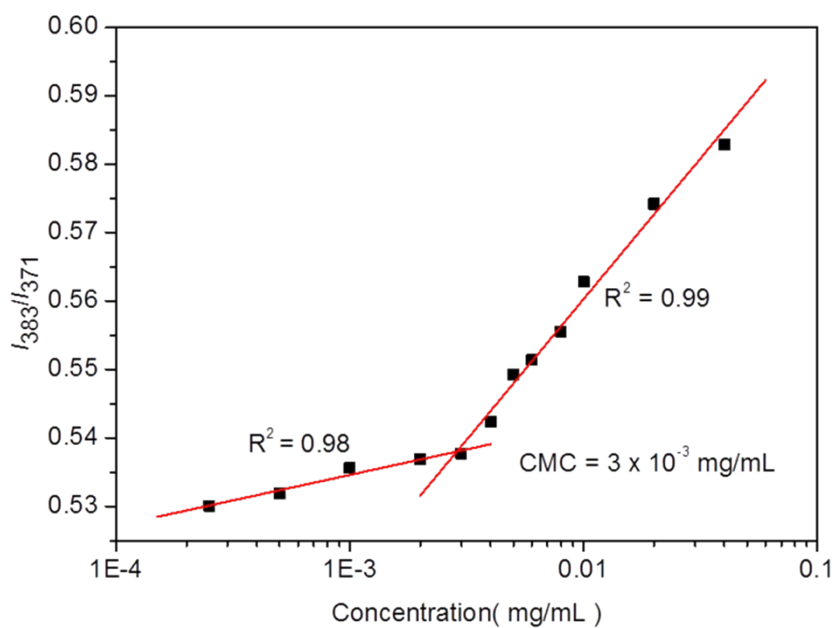


Fig. S21 Plot of the I_{382}/I_{372} ratio with different concentrations of PEG-P[5]A /TPPC6-SS-Py micelles.

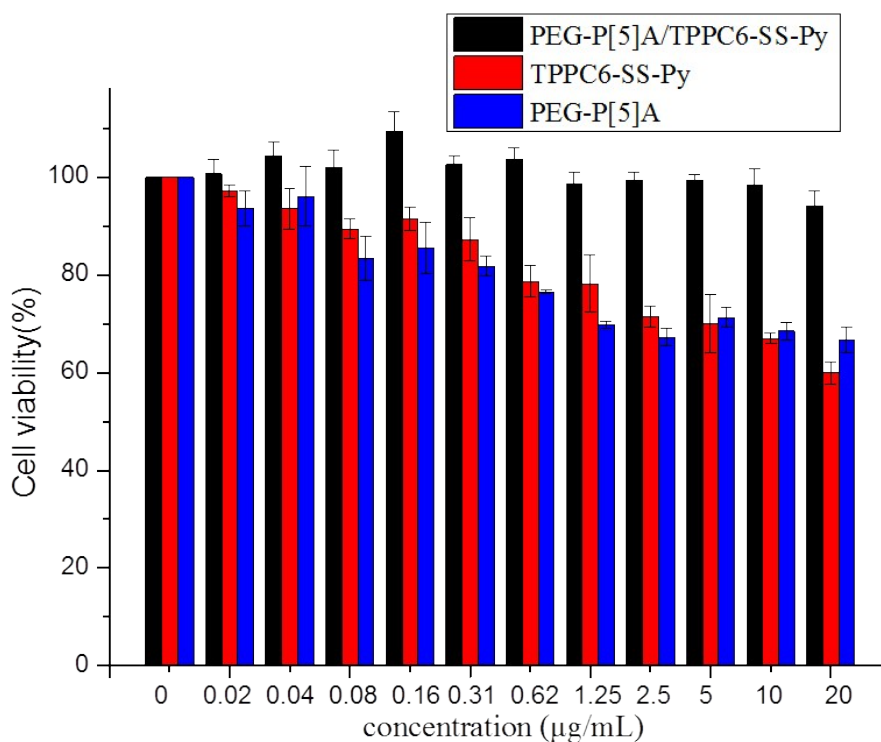


Fig. S22 Viability of A549 cells measured by the MTT assay after treating with different concentration of PEG-P[5]A/TPPC6-SS-Py, TPPC6-SS-Py and PEG-P[5]A without light irradiation.

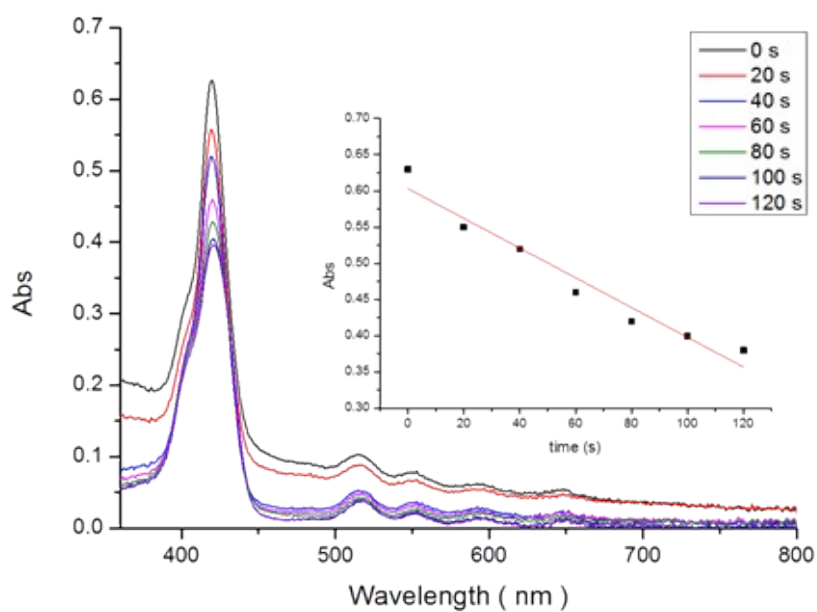


Fig. S23 UV-Vis absorption spectra of DPBF with supramolecular micelles after irradiation for different times (inset: plot of absorbance versus concentration).

References

1. L. Rui, L. Liu, Y. Wang, Y. Gao and W. Zhang, *ACS Macro Lett.*, 2016, **5**, 112-117.
2. F. Liu, Y. Ma, L. Xu, L. Liu and W. Zhang, *Biomater. Sci.*, 2015, **3**, 1218-1227.
3. Q. Duan, Y. Cao, Y. Li, X. Hu, T. Xiao, C. Lin, Y. Pan and L. Wang, *J. Am. Chem. Soc.*, 2013, **135**, 10542-10549.